Proceedings of the Sixth International Conference on
Railway Technology: Research, Development and Maintenance
Edited by: J. Pombo
Civil-Comp Conferences, Volume 7, Paper 2.10
Civil-Comp Press, Edinburgh, United Kingdom, 2024
ISSN: 2753-3239, doi: 10.4203/ccc.7.2.10

Detailed Contact Geometry Processing for 3D Wheel and Rail Surfaces

E. Vollebregt

Vtech CMCC, Rotterdam, The Netherlands

Abstract

The CONTACT software is extended to incorporate the full 3D shape of rails and wheels in the simulation of vehicle-track interaction, covering on the one hand rails with longitudinal profile variation (switches and crossings, turnouts), and on the other hand localized defects like wheel flats and squats. The new version of CONTACT is embedded in SIMPACK Rail using on-line integration, replacing the original methods used for the wheel-rail contact force calculation. A measured wheel flat is taken as an example, computing the impact forces for a range of circumstances. Whereas previous works typically applied a radius variation across the whole width of the wheel, the full 3D shape of the flat is included here accounting for the actual flat depth at the lateral positions on the wheel where contact occurs. The detailed stress histories computed may be used to study the evolution of the wheel flat in time.

Keywords: wheel-rail contact, vehicle-track interaction, multi-body simulation, contact geometry, contact detection, wheel flat.

1 Introduction

Pressed by the large number of time steps used in simulations of vehicle-track interaction (VTI), the true shapes of wheels and rails are typically simplified in the calcu-

lation of the wheel-rail contact forces. The vast majority of contact algorithms require a constant lateral cross-section of the rail and the wheel, where the rail is prismatic and the wheel a body of revolution, see e.g. [1] and the references therein. Extensions were made to support rails with a varying cross-section, especially for the simulation of turnouts, switches and crossings [2, 3] or to support out-of-roundness and corrugation [4, 5]. However, these extensions are typically based off existing algorithms for contact analysis, inheriting part of the restrictions and simplifications of the existing approaches.

This work aims to incorporate the true 3D shapes of wheels and rails generically and fully in the CONTACT software for wheel-rail contact evaluation. The first group of scenarios considered are rails with longitudinal profile variation, as needed for turnouts, switches and crossings, and measured profiles in curves with varying degrees of wear [6]. A second group of 3D shapes are wheels and rails with localized geometrical deviations, such as wheel flats, squats, spalls, gauge corner collapse, and flattened rail heads, as exemplified in Figure 1 (a)–(d). Thirdly, we are interested in harmonic fluctuations along the rail or circumference of the wheel, i.e. corrugation and polygonization (Figure 1 (e)–(f)).

One of the crucial challenges to support these 'fully 3D shapes', not having a constant lateral cross-section, lies in selecting an appropriate surface representation approach. Different strategies may be adopted such as using a triangulation or gridded

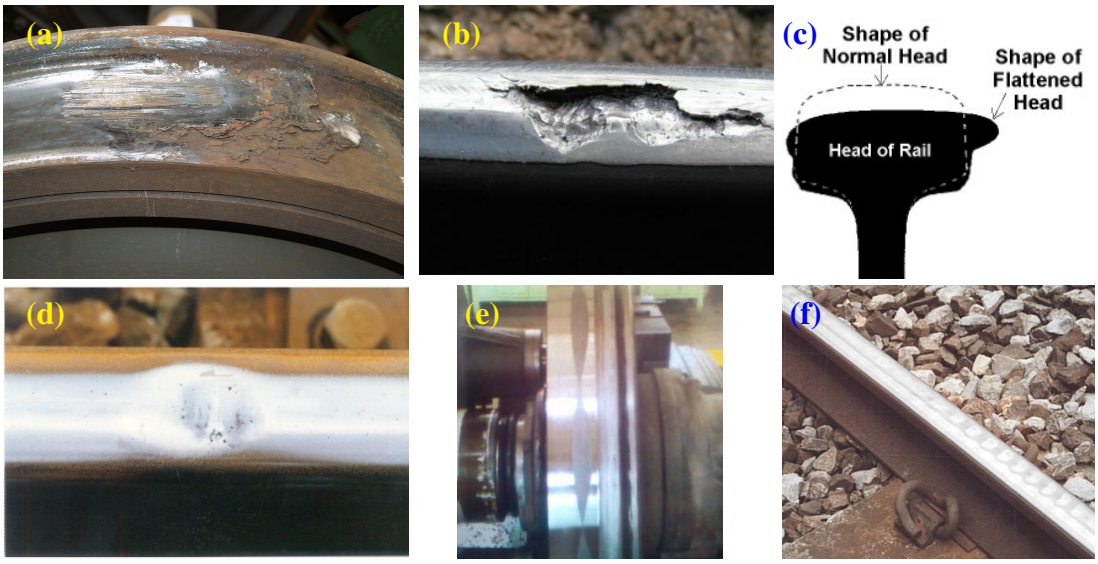

Figure 1: Examples of 3D profile deviations: (a) wheel flat (Wikipedia), (b) gauge corner collapse (Magel, [7]), (c) flattened rail head (NTSB, [8]), (d) squat (Magel, [7]), (e) wheel polygonization (Tao, [9]), (f) rail corrugation (Grassie).

data or using spline surfaces [10]. This choice affects many aspects of the simulation approach, including the possible algorithms for locating contact patches and the quality of the computed results. This paper proposes a framework that lets us discuss these

issues and that aids in structuring of the resulting software.

Another challenge for 3D profile shapes lies in the close interaction of the contact geometry with the vehicle and track dynamics. For instance when a wheel flat enters into the contact zone, the rail moves up while the wheel drops down, creating a sudden impact with possible loss or increase of lateral guiding forces. These dynamics should be accounted for by embedding the contact model in a simulation for vehicle-track interaction. This is achieved by integration of CONTACT in SIMPACK Rail. Simulations were made for a measured wheel flat in different configurations, showing the level of detail provided by a full 3D approach.

This paper is structured as follows. Section 2 discusses alternative methods for 3D geometry modelling. After this follow the choices made for CONTACT and the integration of CONTACT in SIMPACK Rail (Section 3). Results are presented in Section 4, showing the efficacy of the approach, and Section 5 presents the final conclusions.

2 Framework for software organization

One of the crucial challenges to support 'fully 3D shapes', not having a constant lateral cross-section, lies in selecting an appropriate surface representation approach. Different strategies may be adopted as surveyed by Lin and Gottschalk [10]:

a. using a polygonal model, such as a triangulation;

b. using a constructive modeling approach, based on primitives like planes and arcs and associated operations;

c. using a parametric surface, in particular using spline surfaces.

Each of these methods is used in the railway field for 2D profile representation: (a) using tabulated points $\{(y_i, z_i)\}$ with linear interpolation, (b) building a profile from straights and circular arcs, (c) using a parametric spline representation. In 3D, (a) scattered measurement data are processed most easily using triangulation; (b) switch rail geometries may be defined using a base profile and a milling path of a profiling tool [11], (c) spline surfaces are used for switches and crossings [2, 3]. The different strategies may even be recognized in approximate contact methods: (a) adding gridded offsets δz_{ij} for a wheel flat to the wheel-rail distances z_{ij} [4], (b,c) using a constant lateral cross-section at changing height $r_{nom} + \delta r(\theta)$, or evaluating a spline surface using a 'locally prismatic' approach [6].

The choice of the geometry representation affects the quality of the surface model, for instance approximating profile sections using a constant curvature, or splines exhibiting overshoot at sudden changes in curvature [12]. The geometry representation also affects the computed results of the contact model, for instance showing facets obtained from linear interpolation [1]. The range of algorithms for locating contact patches depends on the operations that can be performed efficiently: it is much easier to intersect planes than spline patches. The geometry representation further affects

the user in the ease of use regarding preparation of input data. Different choices may therefore be appropriate in different circumstances, dependent on the scope of the modelling system and the balance between speed and generality of the approach.

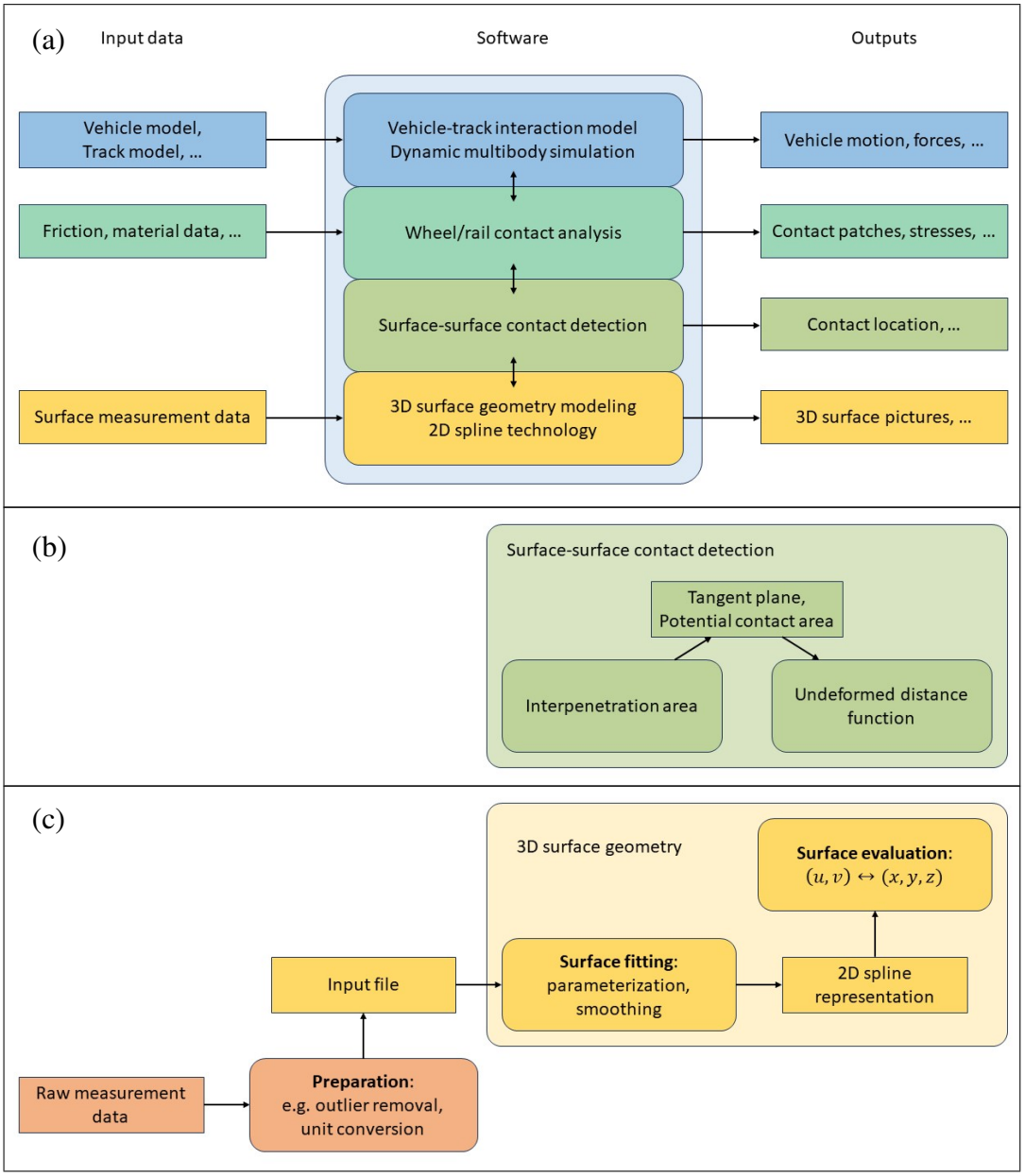

Figure 2: (a) Software organization identifying and separating different tasks in a full vehicle-track interaction simulation. (b) Planar contact analysis revolves around a 'tangent plane'. (c) The 'surface geometry' component consists of 'surface fitting' and 'surface evaluation'.

A framework is introduced that aids in discussing the choices regarding surface geometry, contact analysis, and vehicle-track simulation. In this framework, four components are distinguished as illustrated in Figure 2 (a).

1. Vehicle-track interaction evaluates the dynamics of vehicle and track components. In a time-domain simulation, this concerns the forces acting between different components of the system, and time-integration of the dynamic equations of motion.

2. Wheel-rail contact analysis is considered a specialized topic that should be separated from the main multi-body analysis. Its task is to determine the contact forces and moments as needed by a time-domain simulation. Along the way, this determines contact patches and contact stresses that go into wear and damage calculations.

3. Within the contact analysis, a separate task is identified for determining where the undeformed wheel and rail bodies are contacting each other. In the railway field this is typically called the contact geometry stage [13], identifying the contact location and tangent plane for the subsequent calculation of the contact forces. In Figure 2, this task is called 'surface-surface contact detection'.

4. A cornerstone for contact detection is provided by '3D surface geometry modeling'. How surfaces are represented and stored in the computer is both enabling and limiting the other tasks.

The vertical arrows between the different tasks concern each module's interfaces. These interfaces depend on the methods employed on each side. For instance, the multi-body model may need just the contact forces and their locations if an elastic contact formulation is employed, while additional information may be needed in a constraint force formulation, esp. regarding curvatures at the contact location [13, 14]. Additionally there's freedom as to how responsibilities are partitioned between different tasks. For example it is a matter of choice if total forces are exchanged or separate forces for individual contact patches. This is accommodated for in the CONTACT library version by providing different access routines for 'global' and 'local' forces.

When using a planar contact approach, the 'wheel/rail contact analysis' task starts from a tangent plane defined using a reference position and corresponding reference angle [1]. Further inputs concern the surfaces' interpenetration. A potential contact area is used in CONTACT that is based on the extent of the interpenetration regions. The contact geometry is analyzed twice, first for the location and extent of contact patches, and then for the local geometry of the contact patches [1]. These steps are assigned to the 'contact detection' component as shown in Figure 2 (b).

Two strategies have been implemented in CONTACT for contact detection: a grid-based approach and a method using the contact locus [1]. The contact locus method is based on the notion that the maximum interpenetration of the surfaces needs equal slopes for the wheel and the rail, $\partial z^w/\partial x = \partial z^r/\partial x$. This is used to reduce the complexity of the search, restricting attention to a curve instead of a surface. The method is effective for wheel/rail and wheel/roller contact with constant profiles [1]. It does not work so well in the application to switches and crossings [6]. The reason is that the slope $\partial z^r/\partial x$ need not be monotonous at any fixed y-position. This makes

it hard to find a robust and efficient iteration scheme to determine the equal slope position. The same holds even stronger for discrete profile deviations. The grid-based method is therefore selected as the method of choice for the contact search with discrete profile deviations. Figure 3 gives a basic introduction to this with an eye on surface evaluation.

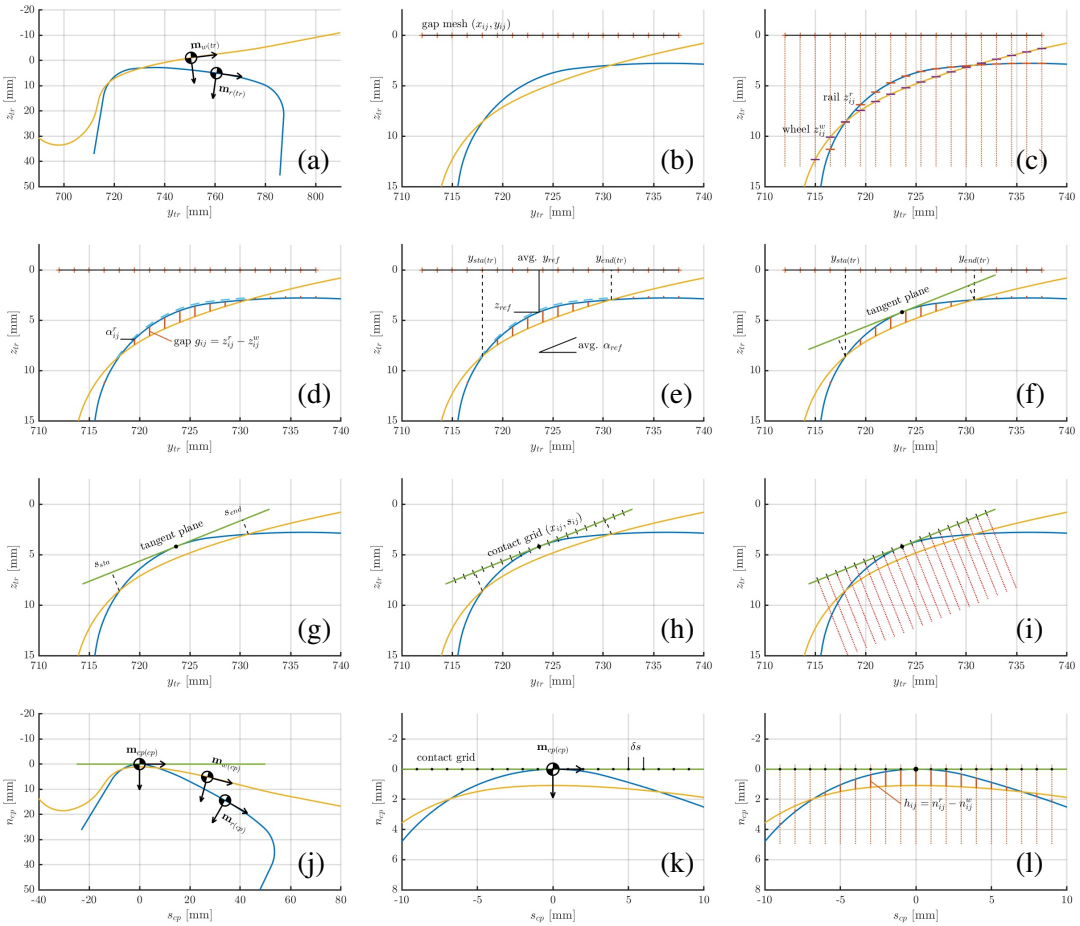

Figure 3: Graphical illustration of the grid-based contact search [1]. (a)–(e) Locating interpenetration areas. (e)–(h) Defining the potential contact area. (i)–(l) Computing the undeformed distance function.

Insight in the roles of ‘surface geometry’ and ‘contact detection’ is gained by considering use of the G+SMO open source software [15]. G+SMO (pronounced ‘gismo’) provides powerful spline technologies for 3-dimensional surface modeling that go far beyond the common tensor spline surface. In particular using NURBS for the description of circular arcs, and using local refinement (THB-splines) for capturing the fine details of the geometry at modest cost of computational time [15]. An effort was made to use G+SMO as a replacement for CONTACT’s internal spline implementation. Two different approaches were considered, using G+SMO just for the surface geometry task or to perform contact detection also in G+SMO.

Delegating the surface geometry to G+SMO involves linking the G+SMO dll into CONTACT, loading the surfaces from appropriate XML input-files, and interrogating the resulting objects as needed in the grid-based contact detection. The interface between CONTACT and G+SMO goes via the functions that are provided on the `gsGeometry` class. A difficult operation is to compute the surfaces' heights z_{ij} for a grid $\{x_{ij}, y_{ij}\}$ on a user-defined plane, used in steps (c) and (i) of Figure 3. Newton iteration is used to find surface parameters (u_{ij}, v_{ij}) on the surfaces at the (x_{ij}, y_{ij}) coordinates provided. Convergence is poor at locations with unfavorable surface curvature. From the side of G+SMO it would be much easier to work with surface parameters (u, v) directly. This shows how the surface model and contact search are interdependent on each other.

From the perspective of CONTACT, it would be convenient to delegate contact detection to G+SMO as well. Generic algorithms for collision detection are available from the literature on computer graphics [10, 16] that go well with the functionality provided by G+SMO. However, CONTACT appears to have non-standard needs with respect to the outcome. The contact reference position and reference angle are based on integrals over the interpenetration region. This is another example of how the interfaces per task depend on the methods employed on either side.

A final take-away from the G+SMO developers is the distinction between different tasks in the 'surface geometry' component as shown in Figure 2 (c). At the core lies a spline surface representation that breaks the component into one part for creating the spline, fitting the given input data, and another part for using the spline for surface evaluation. Many techniques exist for for surface fitting, see e.g. [17, 18] and the references therein. An important aspect concerns the initial parameterization: assigning to each data point (x_{ij}, y_{ij}, z_{ij}) appropriate surface parameters (u_{ij}, v_{ij}), where different choices may lead to different surface approximation. We have been using this implicitly in our previous work on switches and crossings, using 'geometrical features' to define 'interpolation paths' at constant v [6].

3 Implementation in CONTACT

Support is added to the CONTACT software for the detailed modeling of wheel out-of-roundness. Generic algorithms are used to analyze the wheel-rail contact geometry based on a full 3-dimensional wheel representation, capable of predicting contact at any location along the wheel's surface. This development is part of a project supported by the US Federal Railroad Administration (FRA).

The surface for an out-of-round wheel is input to CONTACT using a wheel slices-file with `slcw` filename extension. Wheel slices-files are structured similarly as rail slices-files that were introduced previously for modelling of switches and crossings [6], placing separate lateral cross-sections in separate files, except that longitudinal s_{fc} positions along the track curve are replaced by angles $\theta_{wc} \in [-\pi, \pi)$ around the circumference of the wheel, and vertical heights z are replaced by radial heights dr

with respect to the nominal radius.

A tensor product spline is used that maps a 2-dimensional parameter space (u, v) to a 3-dimensional physical space (θ, y, dr). We standardize on using u for the longitudinal direction (x or θ) and v for the lateral direction (y and z). The spline approximation needs to work in cylindrical coordinates (θ, r) rather than converting the inputs to cartesian (x, z) coordinates and using these in the spline construction. This is because a circle cannot be represented fully using cubic splines, introducing out-of-roundness when using (x, z) as input to the spline construction. Cartesian coordinates could be introduced by adopting NURBS instead of cubic splines. Cylindrical coordinates are more natural though for the wheel surface representation.

Splines are used where the first parameter u is mapped identically into the first physical dimension, $u = x$ for rails and $u = \theta$ for wheels. These are called 'half-parametric splines' with $x = x(u)$, as opposed to 'full-parametric splines' where $x = x(u, v)$. Half-parametric splines simplify inverse evaluation, determining (u, v) at a prescribed (x, y) grid position in steps (c) and (i) of Figure 3.

Wheels with out-of-roundness cannot be computed using the contact search method based on the contact locus. CONTACT automatically switches to use the grid-based method instead. This grid-based contact search is rather slow due to the large number of inverse spline evaluations. New contact search methods are needed to speed up this calculation.

Further extensions are made to CONTACT to enable non-steady rolling in 'module 1' for wheel-rail contact. Whereas the assumption of steady rolling permitted each time-step to be solved independently, a non-steady contact approach requires each time-step to be connected to a previous case. The main ingredients to make this work are the introduction of a super-grid to align the grids used in successive cases, and adding a procedure to establish the connection of new contact patches to the contact patches of the previous case.

A user subroutine is established that provides an interface between CONTACT and SIMPACK Rail. This is used to replace wheel-rail contact forces computed by SIMPACK's internal algorithms by contact forces computed by CONTACT. Interfacing takes place in SIMPACK's time integration, including the interaction of contact forces and dynamic motion. The user subroutine provides access to Kalker's full theory for rolling contact, including extensions for elasto-plastic third body layers, conformal contact, non-steady contact, and detailed handling of wheel flats and switches and crossings.

The new user subroutine is used as a replacement for one or more rail-wheel pairs defined in the SIMPACK model. The original rail-wheel pair needs to be kept in the model such that CONTACT can access its information, especially the rail and wheel state parameters and the profiles used. The forces of the rail-wheel pair are disabled by reducing its elastic modulus E to a tiny value. An auxiliary input-file is used to override hard-coded defaults of the user subroutine and to configure specialized features of CONTACT, see Figure 4 for an example. Non-steady contact is achieved using a sort of co-simulation approach, with SIMPACK and CONTACT marching

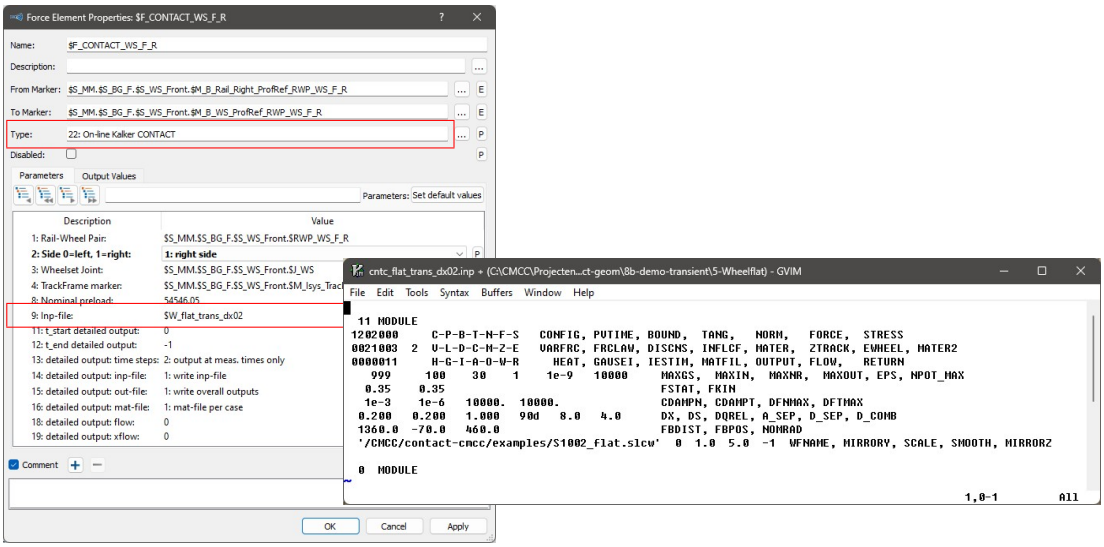

Figure 4: Dialog box for the Kalker CONTACT force element in SIMPACK Rail, using an auxiliary input-file to access the advanced features of CONTACT.

forward in time together. In this case, CONTACT requires that the contact grid moves no more than one or two grid spaces per time step, imposing a time step restriction $\delta t \leq 2\delta x/V$.

4 Wheel flat simulation

A demonstration of the new technologies is made using a measured wheel flat with rounded edges with a length of $160\,\mathrm{mm}$ and maximum depth of $1.4\,\mathrm{mm}$. Geometry measurements were obtained by means of 3D laser scans with $0.03\,\mathrm{mm}$ resolution, post-processed to a uniform grid with steps of $1\,\mathrm{mm}$ in circumferential and lateral directions [19]. These data were kindly provided thanks to prof. Nielsen of Chalmers University of Technology.

The vehicle and track models used are those of the switch and crossing benchmark [2, 20], i.e. the passenger vehicle from the Manchester Benchmarks for rail vehicle simulation and a co-running system of rails and track masses modelled independently between different wheelsets. The SIMPACK models used here are derived from the ones used by Dassault Systèmes in their contribution to the S&C benchmark, kindly provided thanks to Govind Mohan. Switch and guard rails were removed from these models, leaving just UIC60 rails without cant in upright position. Masses and stiffnesses are used according to the S&C benchmark definition [20].

The wheel flat is placed on one side (right wheel) on the leading axle. Simulations are carried out at different velocities $V = 1$ to $200\,\mathrm{m/s}$ for a distance of $6.7\,\mathrm{m}$, comprising three events of the wheel flat on the rail. Each event consists of the right wheel unloading and dropping down, introducing slight roll and yaw rotations of the wheelset, the rail and sleeper bouncing up on the preload force, regaining contact,

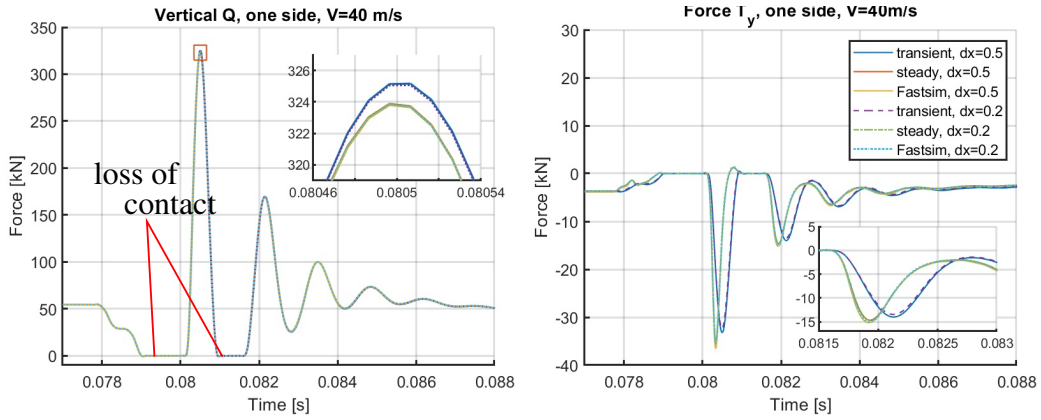

Figure 5: Time histories of vertical force Q and lateral creep force T_y during one wheel flat passage at $V = 40\,\mathrm{m/s}$.

after which mild or fierce dynamic fluctuations are found dependent on the vehicle velocity, masses and stiffnesses used in the simulation.

Initial simulations were made at a vehicle velocity $V = 40\,\mathrm{m/s} = 144\,\mathrm{km/h}$ with results depicted in Figure 5. This shows that the total forces are resolved fully at grid element sizes $\delta x = \delta s = 0.5\,\mathrm{mm}$, with curves on top of the results for $0.2\,\mathrm{mm}$ element sizes. The same dynamics are obtained from Fastsim as for the 'full theory' using the steady rolling approach. The transient rolling method shows a slower build-up of the creep forces resulting in a slight increase of the maximum impact force.

Using a commodity laptop, total calculation times were around 19, 36 and 10 minutes for Fastsim, steady and transient rolling with grid size $0.5\,\mathrm{mm}$. For Fastsim, this time is dominated by the geometrical analysis (75%) and normal contact problem (11%). CONTACT's KPEC method could not be used because of discrete jumps in its outputs interfering with SIMPACK's adaptive time stepping method. The good performance of the transient contact method comes from the number of time steps used, halved compared to the run using Fastsim, and from using the TangCG solver instead of SteadyGS [21, 22]. The main contributions to the total time come from the geometrical analysis (59%) and the normal and tangential solvers (10%, 21%).

The maximum impact force is shown in Figure 6 (left) for velocities up to $200\,\mathrm{m/s}$ or $720\,\mathrm{km/h}$. This large range is used to establish the downward trend at high velocity that was predicted but not clearly visible in Pieringer's results [4]. The time histories show a combination of rapid and slower fluctuations corresponding to the P1 and P2 forces (Figure 6 (right)). Additional simulations verified that the maximum value and corresponding velocity depend on the masses and stiffnesses used. The local maximum found just below $10\,\mathrm{m/s}$ may correspond to the pronounced local maximum found by Pieringer et al. From the time series we suspect that this local maximum comes from superposition of P1 and P2 fluctuations.

Detailed results on the contact patches and contact pressures p_n are shown in Figure 7 for the simulation at $V = 6\,\mathrm{m/s}$ at eight wheelset pitch angles θ_{ws}. In the bottom

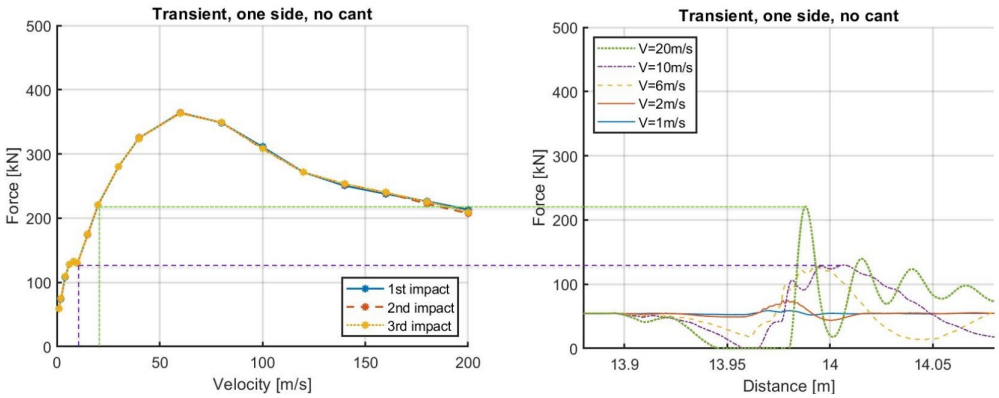

Figure 6: Left: maximum impact force in simulations with a wheel flat on one side of a vehicle's leading axle. Right: wheel unloading, regaining contact, and fluctuations of vertical load Q at low to medium velocities.

part of the figure, the forward direction of the wheel is in upward direction in the figure. The location of the wheel flat is indicated by the grey contour lines. As the wheel rolls forward, the contact grid moves up, and the wheel surface moves down through the picture. The dark-red contour shows the outline of the contact patch for a round wheel with nominal profile. From this we see how the contact patch shifts back at first, moves sideways and then advances ahead of the nominal patch, after which it finally comes back to the reference shape and position.

Figure 7 shows the deepest part of the wheel flat staying to the right of the nominal contact position. That is, the wheel flat does not strike the rail fully in this simulation. The flat depth experienced in the simulation is less than the maximum depth at the center of the flat. This is accounted for fully in the simulation, including shift and roll of the rail, and including the wheelset lateral shift, roll and yaw motion. In the current situation, one contributing factor is the absence of rail cant, moving the nominal contact patch towards the gauge corner compared to a canted rail placement. Additional simulations with $1:40$ cant show contact patches at the crown of the rail, increasing the maximum impact force by 27% to $\max(Q) = 462\,\mathrm{kN}$ at $V = 60\,\mathrm{m/s}$.

5 Conclusions and discussion

This paper presented work on incorporating the true 3D wheel and rail surface shapes into simulations of vehicle-track interaction, producing detailed pictures of the evolution of the contact stresses.

The main challenge was found in selecting a 3D surface representation approach and corresponding algorithm for location of contact patches. Techniques were surveyed from the fields of Computer Graphics and Computer-Aided Geometrical Design, resulting in a modular design for the VTI software organization. A half parametric spline surface is adopted in CONTACT based on lateral slices. The u parameter

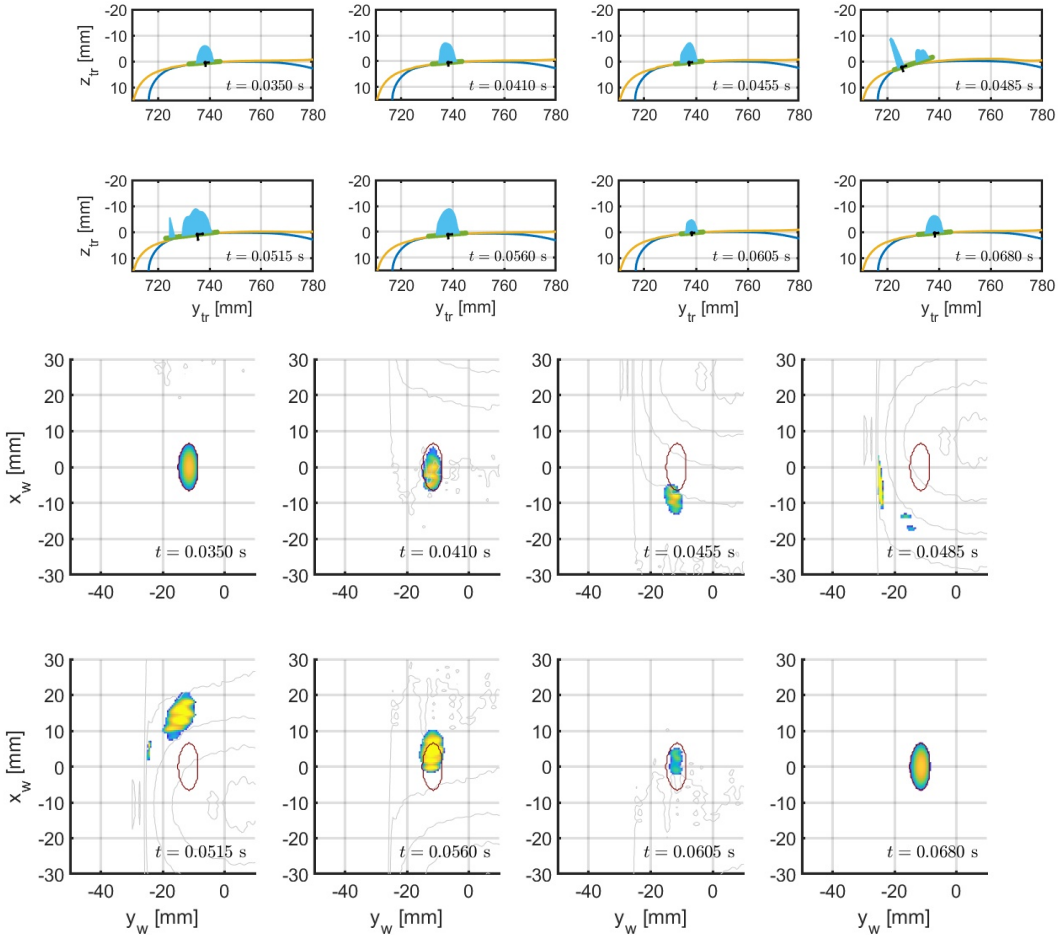

Figure 7: Contact patches and pressures in rear view and top view at selected time instances t in the wheel flat simulation at $V = 6\,\mathrm{m/s}$.

is aligned strictly with the longitudinal direction x or θ, facilitating the grid-based contact search approach.

The CONTACT software was extended with respect to non-steady contact analysis and integrated in SIMPACK Rail using a user subroutine. Simulations were presented for a wheel with a measured flat. The 3D approach shows how the contact patch moves backward and forward on the flanks of the flat and how the dynamics are altered if the flat is partially missed, not struck at its deepest contour. Non-steady contact calculations show slower build-up of tangential forces than are predicted using the steady rolling assumption.

Further work is needed on preprocessing of measured surface data, e.g. outlier removal and smoothing, and speed up of the calculations.

Acknowledgements

This work has been supported by the US Federal Railroad Administration under contracts 693JJ622C000008 and 693JJ622C000017. Thanks to prof. Nielsen of Chalmers University of Technology for providing the wheel flat measurement data. Thanks to Govind Mohan (Dassault Systèmes) for the SIMPACK models used in the switch and crossing benchmark.

References

[1] E.A.H. Vollebregt. Detailed wheel/rail geometry processing using the planar contact approach. *Vehicle System Dynamics*, 60(4):1253–1291, 2022. Open access.

[2] Y. Bezin, B.A. Pålsson, W. Kik, P. Schreiber, J. Clarke, V. Beuter, M. Sebes, I. Persson, H. Magalhaes, P. Wang, and P. Klauser. Multibody simulation benchmark for dynamic vehicle-track interaction in switches and crossings: results and method statements. *Vehicle System Dynamics*, 61(3):660–697, 2023.

[3] Repository for participants' method statements. University of Huddersfield, 2021. https://doi.org/10.34696/s60x-ay18.

[4] A. Pieringer, W. Kropp, and J.C.O. Nielsen. The influence of contact modelling on simulated wheel/rail interaction due to wheel flats. *Wear*, 314(1-2):273–281, 2014.

[5] S.D. Iwnicki, J.C.O. Nielsen, and G.Q. Tao. Out-of-round railway wheels and polygonisation. *Vehicle System Dynamics*, 61(7):1787–1830, 2023.

[6] E.A.H. Vollebregt, P. Klauser, A. Keylin, P. Schreiber, D. Sammon, and N. Wilson. Extension of CONTACT for switches and crossings and demonstration for S&C benchmark cases. In W. Huang and M. Ahmadian, editors, *The 28th IAVSD Symposium on Dynamics of Vehicles on Roads and Tracks (IAVSD2023)*, Lecture Notes in Mechanical Engineering, page paper 236, Cham, 2023. Springer.

[7] E.E. Magel. Rolling contact fatigue: A comprehensive review. Technical Report DOT/FRA/ORD-11/24, Federal Railroad Administration, November 2011.

[8] NTSB. Railroad accident report – Derailment of Amtrak train 49 on Conrail trackage near Batavia, New York, on August 3, 1994. Technical Report NTSB/RAR-96/02, NTSB, Washington, DC 20594, 1996.

[9] G. Tao, Z. Wen, G. Chen, Y. Luo, and X. Jin. Locomotive wheel polygonisation due to discrete irregularities: field measurement, simulation and mechanism. In M. Klomp, F. Bruzelius, J. Nielsen, and A. Hillemyr, editors, *Advances in Dynamics of Vehicles on Roads and Tracks. IAVSD 2019*, page paper 26, Cham, 2020. Springer.

[10] M.C. Lin and S. Gottschalk. Collision detection between geometric models: a survey. In *IMA Conference on Mathematics of Surfaces, San Diego, CA*, volume 1, pages 602–608, 1998.

[11] B.A. Pålsson. Design optimisation of switch rails in railway turnouts. *Vehicle System Dynamics*, 51:1619–1639, 2013.

[12] E.A.H. Vollebregt, A. Darbani, A. Ashtekar, and K. Oldknow. Smoothing procedures for detailed wheel/rail geometry processing. In P. Meehan and W. Yan et al., editors, *Proceedings of the 12th International Conference on Contact Mechanics and Wear of Rail/Wheel Systems*, pages 1–7, Australia, 2022. Monash University.

[13] E.A.H. Vollebregt. Detailed wheel/rail geometry processing using the conformal contact approach. *Multibody System Dynamics*, 52:135–167, 2021. Open access.

[14] A.A. Shabana, K.E. Zaazaa, and H. Sugiyama. *Railroad Vehicle Dynamics: A Computational Approach*. CRC Press, Boca Raton, 2008.

[15] G. Kiss, C. Giannelli, U. Zore, B. Jüttler, D. Großmann, and J. Barner. Adaptive CAD model (re-)construction with THB-splines. *Graphical Models*, 76(5):273–288, 2014.

[16] P. Jiménez, F. Thomas, and C. Torras. 3D collision detection: a survey. *Computers and Graphics*, 25:269–285, 2001.

[17] M. Desbrun, M. Meyer, and P. Alliez. Intrinsic parameterizations of surface meshes. *Computer Graphics Forum*, 21:1–10, 2002.

[18] V. Weiss, L. Andor, G. Renner, and T Várady. Advanced surface fitting techniques. *Computer Aided Geometric Design*, 19:19–42, 2002.

[19] M. Maglio, T. Vernersson, J.C.O. Nielsen, A. Ekberg, and E. Kabo. Influence of railway wheel tread damage on wheel-rail impact loads and the durability of wheelsets. *Railway Engineering Science*, 2023.

[20] Y. Bezin and B.A. Pålsson. Multibody simulation benchmark for dynamic vehicle-track interaction in switches and crossings: modelling description and simulation tasks. *Vehicle System Dynamics*, 61(3):644–659, 2023.

[21] J. Zhao, E.A.H. Vollebregt, and C.W. Oosterlee. A fast nonlinear conjugate gradient based method for 3D concentrated frictional contact problems. *J. of Computational Physics*, 288:86–100, 2015.

[22] E.A.H. Vollebregt. Improving the speed and accuracy of the frictional rolling contact model "CONTACT". In B.H.V. Topping, J.M. Adam, F.J. Pallarés, R. Bru, and M.L. Romero, editors, *Proceedings of the 10th International Conference on Computational Structures Technology*, pages 1–15, Stirlingshire, United Kingdom, 2010. Civil-Comp Press. DOI: 10.4203/ccp.93.17.